observed by LSCM as previously described (17). For flow cytometric analysis, macrophages stained with LysoTracker were washed with PBS and suspended in PBS containing 1% FBS. Flow cytometric analysis was performed on a FACSAria flow cytometer (BD Bioscience). For labeling lysosomal vesicles with fluorescent dextran, cells were incubated with Texas Red-dextran (Invitrogen) at 100 μg/mL for 8 h, followed by washing and chasing in fluorescent-dextran-free DMEM with 10% FBS for 16 h. Immunofluorescence microscopy was performed as previously described (17). For quantification of fluorescence, serial confocal sections at 0.5 μm steps within a *z*-stack spanning a total thickness of 12 μm were taken, and *z*-stacks were collapsed into a single *x*–*y* projection. The accumulation of LysoTracker, cathepsin D and fluorescent dextran within the phagosome and other E/L components was quantified by ImageJ using collapsed fluorescent images. Fluorescent density was calculated as that the fluorescent intensity is divided by the area.

Plasmid constructs and transfection

PCR was carried out using cDNA derived from HeLa cells as a template and the primer sets were listed in Table S2. PCR products of the amplified Rab GTPase genes were inserted into the pEGFP-C1 (Invitrogen) or pCI (Promega) vectors. CA and DN mutants of Rab GTPases were prepared by site-directed mutagenesis as described previously (50,51) using the primer sets listed in Table S3. Transfection of cells with plasmid was performed as described previously (17). Briefly, two million cells of Raw264.7 macrophages were transfected with 10 μg of plasmid DNA using an MP-100 electroporator (Digital Bio Technology), according to the manufacturer's instructions. Transfected cells were incubated in DMEM with 10% FBS for 24 h prior to the experiments.

Statistics

The unpaired or paired two-sided Student's *t*-test was used to assess the statistical significance of differences between the two groups. Tukey–Kramer multiple comparison test was used for the assessment of the statistical significance of differences among three groups. For the assessment of the differences of the proportions of fluorescence-positive phagosomes, we did three independent experiments and counted more than 100 phagosomes at each condition. Assessment of the differences in fluorescent density accumulating within the phagosomes was conducted over three independent experiments, with more than 100 phagosomes examined for each condition.

Acknowledgments

We thank Drs Toshi Nagata and Masato Uchijima (Hamamatsu University School of Medicine, Hamamatsu, Japan) for their helpful discussions. We also thank Ms Yumiko Suzuki (Hamamatsu University School of Medicine) for her excellent assistance. This work was supported in part by Grants-in-Aid for Young Scientists (B) and Scientific Research (B and C) from the Japan Society for the Promotion of Science; Scientific Research on Priority Areas from the Ministry of Education, Culture, Sports, Science and Technology of Japan; the Health and Labour Science Research Grants for Research into Emerging and Reemerging Infectious Diseases from the Ministry of Health, Labour and Welfare of Japan and the United States-Japan Cooperative Medical Science Committee.

Supporting Information

Additional Supporting Information may be found in the online version of this article:

Figure S1: Localization of Rab GTPases on *S. aureus*- and *M. tb*-containing phagosomes. The subcellular localization of the Rab GTPases from Figure 2 is shown. Raw264.7 macrophages expressing EGFP-Rab GTPases were infected with *S. aureus* labeled with Texas Red (SA) or *M. tb* expressing DsRed (MTB). Infected cells were fixed at the indicated time-points and observed by LSCM. Left and right panels show images of macrophages with and without images of infected bacteria, respectively. Arrows and arrowheads indicate phagosomes with and without the localization of Rab GTPases, respectively. Scale bar, 10 μm.

Figure S2: Rab GTPases not associated with *S. aureus*-containing phagosomes. The subcellular localization of 20 Rab GTPases are shown. No significant associations with *S. aureus* (A) and *M. tb* (B) were observed at any of the time-points up to 6 h (less than 20% of the phagosomes).

Figure S3: Flow cytometric analysis reveals that expression of the DN forms of Rab GTPases has no influence on the generation of acidic vesicles in macrophages. Macrophages were transfected with expression plasmids for EGFP and the DN forms of Rab GTPases. Transfected cells were stained with 300 nM LysoTracker for 30 min, followed by flow cytometric analysis. The ratio of mean fluorescent intensity derived from GFP-positive cells (Q2) to that from GFP-negative cells (Q4) is indicated. The proportions of cells that were GFP positive (Q2) and negative (Q4) are also indicated.

Figure S4: Localization of Rab5 and Rab10 to the phagosomes. A) Raw264.7 macrophages expressing EGFP-Rab5 were infected with *M. bovis* BCG. B and C) Raw264.7 macrophages expressing EGFP-Rab10 were infected with *S. aureus* (SA) or *M. tb* (MTB). A-1, B-1 and C-1 show subcellular localization of Rab GTPases (Rab5 and Rab10). A-2, B-2 and B-3 show bacteria (BCG, SA and MTB). A-3, B-3 and C-3 show the merged images of macrophage and bacteria (merge). Arrows and arrowheads indicate phagosomes with and without the localization of Rab GTPases, respectively. Scale bar, 10 μm.

Figure S5: Rab GTPases recruited to phagosomes containing *M. tb*. Rab GTPases recruited to phagosomes containing *S. aureus* or *M. tb* are shown. Rab GTPases shown in blue, green or red are involved in phagosomal acidification, cathepsin D recruitment to the phagosomes or both, respectively. Boxed Rab GTPases are dissociated from *M. tb*-containing phagosomes. EE, early endosomes; ER, endoplasmic reticulum; LE, late endosomes; LY, lysosomes; RE, recycling endosomes; TGN, trans-Golgi network.

Table S1: Subcellular localization of Rab GTPases

Table S2: Primer list for construction of plasmid of EGFP-fused Rab GTPases

Table S3: Primer list for site-directed mutagenesis

Please note: Wiley-Blackwell are not responsible for the content or functionality of any supporting materials supplied by the authors. Any queries (other than missing material) should be directed to the corresponding author for the article.

References

1. Vieira OV, Botelho RJ, Grinstein S. Phagosome maturation: aging gracefully. Biochem J 2002;366:689–704.
2. Vieira OV, Botelho RJ, Rameh L, Brachmann SM, Matsuo T, Davidson HW, Schreiber A, Backer JM, Cantley LC, Grinstein S. Distinct roles of class I and class III phosphatidylinositol 3-kinases in phagosome formation and maturation. J Cell Biol 2001;155:19–25.
3. Kitano M, Nakaya M, Nakamura T, Nagata S, Matsuda M. Imaging of Rab5 activity identifies essential regulators for phagosome maturation. Nature 2008;453:241–245.
4. Vieira OV, Bucci C, Harrison RE, Trimble WS, Lanzetti L, Gruenberg J, Schreiber AD, Stahl PD, Grinstein S. Modulation of Rab5 and Rab7 recruitment to phagosomes by phosphatidylinositol 3-kinase. Mol Cell Biol 2003;23:2501–2514.
5. Harrison RE, Bucci C, Vieira OV, Schroer TA, Grinstein S. Phagosomes fuse with late endosomes and/or lysosomes by extension of membrane protrusions along microtubules: role of Rab7 and RILP. Mol Cell Biol 2003;23:6494–6506.
6. Armstrong JA, Hart PD. Response of cultured macrophages to *Mycobacterium tuberculosis*, with observations on fusion of lysosomes with phagosomes. J Exp Med 1971;134:713–740.

7. Clemens DL, Horwitz MA. Characterization of the *Mycobacterium tuberculosis* phagosome and evidence that phagosomal maturation is inhibited. J Exp Med 1995;181:257–270.
8. Russell DG. *Mycobacterium tuberculosis*: here today, and here tomorrow. Nat Rev Mol Cell Biol 2001;2:569–577.
9. Rink J, Ghigo E, Kalaidzidis Y, Zerial M. Rab conversion as a mechanism of progression from early to late endosomes. Cell 2005;122: 735–749.
10. Vergne I, Chua J, Singh SB, Deretic V. Cell biology of *Mycobacterium tuberculosis* phagosome. Annu Rev Cell Dev Biol 2004;20:367–394.
11. Deretic V, Vergne I, Chua J, Master S, Singh SB, Fazio JA, Kyei G. Endosomal membrane traffic: convergence point targeted by *Mycobacterium tuberculosis* and HIV. Cell Microbiol 2004;6: 999–1009.
12. Roberts EA, Chua J, Kyei GB, Deretic V. Higher order Rab programming in phagolysosome biogenesis. J Cell Biol 2006;174:923–929.
13. Vergne I, Chua J, Lee HH, Lucas M, Belisle J, Deretic V. Mechanism of phagolysosome biogenesis block by viable *Mycobacterium tuberculosis*. Proc Natl Acad Sci U S A 2005;102:4033–4038.
14. Via LE, Deretic D, Ulmer RJ, Hibler NS, Huber LA, Deretic V. Arrest of mycobacterial phagosome maturation is caused by a block in vesicle fusion between stages controlled by rab5 and rab7. J Biol Chem 1997;272:13326–13331.
15. Kelley VA, Schorey JS. *Mycobacterium's* arrest of phagosome maturation in macrophages requires Rab5 activity and accessibility to iron. Mol Biol Cell 2003;14:3366–3377.
16. Sun J, Deghmane AE, Soualhine H, Hong T, Bucci C, Solodkin A, Hmama Z. *Mycobacterium bovis* BCG disrupts the interaction of Rab7 with RILP contributing to inhibition of phagosome maturation. J Leukoc Biol 2007;82:1437–1445.
17. Seto S, Matsumoto S, Ohta I, Tsujimura K, Koide Y. Dissection of Rab7 localization on *Mycobacterium tuberculosis* phagosome. Biochem Biophys Res Commun 2009;387:272–277.
18. Seto S, Matsumoto S, Tsujimura K, Koide Y. Differential recruitment of CD63 and Rab7-interacting-lysosomal-protein to phagosomes containing *Mycobacterium tuberculosis* in macrophages. Microbiol Immunol 2010;54:170–174.
19. Kyei GB, Vergne I, Chua J, Roberts E, Harris J, Junutula JR, Deretic V. Rab14 is critical for maintenance of *Mycobacterium tuberculosis* phagosome maturation arrest. EMBO J 2006;25:5250–5259.
20. Schwartz SL, Cao C, Pylypenko O, Rak A, Wandinger-Ness A. Rab GTPases at a glance. J Cell Sci 2007;120:3905–3910.
21. Stenmark H, Olkkonen VM. The Rab GTPase family. Genome Biol 2001;2:REVIEWS3007.
22. Garin J, Diez R, Kieffer S, Dermine JF, Duclos S, Gagnon E, Sadoul R, Rondeau C, Desjardins M. The phagosome proteome: insight into phagosome functions. J Cell Biol 2001;152:165–180.
23. Rogers LD, Foster LJ. The dynamic phagosomal proteome and the contribution of the endoplasmic reticulum. Proc Natl Acad Sci U S A 2007;104:18520–18525.
24. Shui W, Sheu L, Liu J, Smart B, Petzold CJ, Hsieh TY, Pitcher A, Keasling JD, Bertozzi CR. Membrane proteomics of phagosomes suggests a connection to autophagy. Proc Natl Acad Sci U S A 2008;105:16952–16957.
25. Smith AC, Heo WD, Braun V, Jiang X, Macrae C, Casanova JE, Scidmore MA, Grinstein S, Meyer T, Brumell JH. A network of Rab GTPases controls phagosome maturation and is modulated by *Salmonella enterica* serovar Typhimurium. J Cell Biol 2007;176:263–268.
26. Beatty WL, Rhoades ER, Hsu DK, Liu FT, Russell DG. Association of a macrophage galactoside-binding protein with *Mycobacterium*-containing phagosomes. Cell Microbiol 2002;4:167–176.
27. Desjardins M, Huber LA, Parton RG, Griffiths G. Biogenesis of phagolysosomes proceeds through a sequential series of interactions with the endocytic apparatus. J Cell Biol 1994;124:677–688.
28. Brumell JH, Scidmore MA. Manipulation of rab GTPase function by intracellular bacterial pathogens. Microbiol Mol Biol Rev 2007;71:636–652.
29. Clemens DL, Lee BY, Horwitz MA. *Mycobacterium tuberculosis* and *Legionella pneumophila* phagosomes exhibit arrested maturation despite acquisition of Rab7. Infect Immun 2000;68:5154–5166.
30. Fratti RA, Backer JM, Gruenberg J, Corvera S, Deretic V. Role of phosphatidylinositol 3-kinase and Rab5 effectors in phagosomal biogenesis and mycobacterial phagosome maturation arrest. J Cell Biol 2001;154:631–644.
31. Ng EL, Wang Y, Tang BL. Rab22B's role in trans-Golgi network membrane dynamics. Biochem Biophys Res Commun 2007;361:751–757.
32. Wang T, Hong W. Interorganellar regulation of lysosome positioning by the Golgi apparatus through Rab34 interaction with Rab-interacting lysosomal protein. Mol Biol Cell 2002;13:4317–4332.
33. Wasmeier C, Romao M, Plowright L, Bennett DC, Raposo G, Seabra MC. Rab38 and Rab32 control post-Golgi trafficking of melanogenic enzymes. J Cell Biol 2006;175:271–281.
34. Ullrich HJ, Beatty WL, Russell DG. Direct delivery of procathepsin D to phagosomes: implications for phagosome biogenesis and parasitism by *Mycobacterium*. Eur J Cell Biol 1999;78:739–748.
35. Dejgaard SY, Murshid A, Erman A, Kizilay O, Verbich D, Lodge R, Dejgaard K, Ly-Hartig TB, Pepperkok R, Simpson JC, Presley JF. Rab18 and Rab43 have key roles in ER-Golgi trafficking. J Cell Sci 2008;121:2768–2781.
36. Das Sarma J, Kaplan BE, Willemsen D, Koval M. Identification of rab20 as a potential regulator of connexin 43 trafficking. Cell Commun Adhes 2008;15:65–74.
37. Curtis LM, Gluck S. Distribution of Rab GTPases in mouse kidney and comparison with vacuolar H+-ATPase. Nephron Physiol 2005;100:31–42.
38. Lee BY, Jethwaney D, Schilling B, Clemens DL, Gibson BW, Horwitz MA. The *Mycobacterium bovis* bacille Calmette-Guerin phagosome proteome. Mol Cell Proteomics 2010;9:32–53.
39. Philips JA, Porto MC, Wang H, Rubin EJ, Perrimon N. ESCRT factors restrict mycobacterial growth. Proc Natl Acad Sci U S A 2008;105:3070–3075.
40. Kumar D, Nath L, Kamal MA, Varshney A, Jain A, Singh S, Rao KV. Genome-wide analysis of the host intracellular network that regulates survival of *Mycobacterium tuberculosis*. Cell 2010;140:731–743.
41. Vanlandingham PA, Ceresa BP. Rab7 regulates late endocytic trafficking downstream of multivesicular body biogenesis and cargo sequestration. J Biol Chem 2009;284:12110–12124.
42. Vergne I, Fratti RA, Hill PJ, Chua J, Belisle J, Deretic V. *Mycobacterium tuberculosis* phagosome maturation arrest: mycobacterial phosphatidylinositol analog phosphatidylinositol mannoside stimulates early endosomal fusion. Mol Biol Cell 2004;15:751–760.
43. Cox D, Lee DJ, Dale BM, Calafat J, Greenberg S. A Rab11-containing rapidly recycling compartment in macrophages that promotes phagocytosis. Proc Natl Acad Sci U S A 2000;97:680–685.
44. Frigui W, Bottai D, Majlessi L, Monot M, Josselin E, Brodin P, Garnier T, Gicquel B, Martin C, Leclerc C, Cole ST, Brosch R. Control of *M. tuberculosis* ESAT-6 secretion and specific T cell recognition by PhoP. PLoS Pathog 2008;4:e33.
45. Abdallah AM, Gey van Pittius NC, Champion PA, Cox J, Luirink J, Vandenbroucke-Grauls CM, Appelmelk BJ, Bitter W. Type VII secretion – mycobacteria show the way. Nat Rev Microbiol 2007;5: 883–891.
46. Smith J, Manoranjan J, Pan M, Bohsali A, Xu J, Liu J, McDonald KL, Szyk A, LaRonde-LeBlanc N, Gao LY. Evidence for pore formation in host cell membranes by ESX-1-secreted ESAT-6 and its role in *Mycobacterium marinum* escape from the vacuole. Infect Immun 2008;76:5478–5487.
47. Cardoso CM, Jordao L, Vieira OV. Rab10 regulates phagosome maturation and its overexpression rescues *Mycobacterium*-containing phagosomes maturation. Traffic 2010;11:221–235.
48. Aoki K, Matsumoto S, Hirayama Y, Wada T, Ozeki Y, Niki M, Domenech P, Umemori K, Yamamoto S, Mineda A, Matsumoto M, Kobayashi K. Extracellular mycobacterial DNA-binding protein 1 participates in mycobacterium-lung epithelial cell interaction through hyaluronic acid. J Biol Chem 2004;279:39798–39806.
49. Chua J, Deretic V. *Mycobacterium tuberculosis* reprograms waves of phosphatidylinositol 3-phosphate on phagosomal organelles. J Biol Chem 2004;279:36982–36992.
50. Fukuda M, Kanno E, Ishibashi K, Itoh T. Large scale screening for novel rab effectors reveals unexpected broad Rab binding specificity. Mol Cell Proteomics 2008;7:1031–1042.
51. Itoh T, Satoh M, Kanno E, Fukuda M. Screening for target Rabs of TBC (Tre-2/Bub2/Cdc16) domain-containing proteins based on their Rab-binding activity. Genes Cells 2006;11:1023–1037.

Table S1 Subcellular localization of Rab GTPases

	Localization	Acidification[a]	Cathepsin D[b]	LAMP2[c]	References
Rab1	Endoplasmic reticulum	N.T.	N.T.	-	(1)
Rab1b	Endoplasmic reticulum	N.T.	N.T.	-	(1)
Rab2	Endoplasmic reticulum	N.T.	N.T.	-	(1)
Rab2b	Endoplasmic reticulum	N.T.	N.T.	-	(1)
Rab3	Golgi	N.T.	N.T.	-	(2)
Rab3b	Golgi	N.T.	N.T.	-	(2)
Rab4	Early and recycling endosomes	N.T.	N.T.	+	(3)
Rab4b	Early and recycling endosomes	N.T.	N.T.	+	(3)
Rab5	Early endosomes	-	-	-	(4)
Rab5b	Early endosomes	N.T.	N.T.	-	(4)
Rab6	Golgi	N.T.	N.T.	-	(5)
Rab6b	Golgi	N.T.	N.T.	-	(5)
Rab7	Late endosomes, lysosomes	+	+	++	(6)
Rab7b	Late endosomes, lysosomes	-	-	++	(7)
Rab8	Golgi	-	-	-	(8)
Rab8b	Golgi	-	-	-	(8)
Rab9	Late endosomes	-	-	++	(9)
Rab9b	Late endosomes	-	-	++	(9)
Rab10	Golgi, early endosomes	N.T.	N.T.	+	(8, 10)
Rab11	Golgi, recycling endosomes	-	-	+	(11)
Rab11b	Golgi, recycling endosomes	-	-	+	(11)
Rab13	Golgi, plasma membrane	-	-	-	(12), this study
Rab14	Golgi, trans-Golgi	-	-	-	(13)
Rab16	Golgi	N.T.	N.T.	-	(14)
Rab18	Endoplasmic reticulum	N.T.	N.T.	-	(15)
Rab20	Endoplasmic reticulum	+	+	-	(16)
Rab21	Early endosomes	N.T.	N.T.	-	(17)
Rab22a	Early endosomes	-	-	+	(18)
Rab22b	Early endosomes	-	+	-	(19)
Rab23	Plasma membrane	-	-	+	(20)
Rab24	Perinuclear region	N.T.	N.T.	-	This study
Rab27	Lysosomes	-	-	++	(21)
Rab28		N.T.	N.T.	-	
Rab29		N.T.	N.T.	-	
Rab30	Golgi	N.T.	N.T.	-	(15)
Rab32	Golgi, mitochondria	-	+	-	(22)
Rab34	Golgi	-	+	+	(23)
Rab35	Plasma membrane	N.T.	N.T.	-	(24)
Rab37	Lysosomes	-	-	++	(25)
Rab38	Golgi, mitochondria	-	+	-	(22)
Rab39	Perinuclear region and lysosomes	+	-	++	This study
Rab43	Golgi	-	+	-	(15)

(a) Involvement of Rab GTPases in the phagosomal acidification (Figure 4). +; function, -; non-function, N.T.; not tested.
(b) Involvement of Rab GTPases in the recruitment of cathepsin D to the phagoosme (Figure 5). +; function, -; non-function, N.T.; not tested.

(c) Co-localization of Rab GTPases and LAMP2. Raw264.7macrophages transfected with EGFP-fused Rab GTPases were stained with anti-LAMP-2 antibody, followed by observation with lasar scanning confocal microscopy. Pearson's correlation (PC) of overlapping fluorescent areas of EGFP-fused Rab GTPases and LAMP-2 was assessed. -; PC < 0, +; 0 < PC < 0.3, ++; PC > 0.3.

References

1. Tisdale EJ, Bourne JR, Khosravi-Far R, Der CJ, Balch WE. GTP-binding mutants of rab1 and rab2 are potent inhibitors of vesicular transport from the endoplasmic reticulum to the Golgi complex. J Cell Biol 1992;119:749-761.
2. Abu-Amer Y, Teitelbaum SL, Chappel JC, Schlesinger P, Ross FP. Expression and regulation of RAB3 proteins in osteoclasts and their precursors. J Bone Miner Res 1999;14:1855-1860.
3. van der Sluijs P, Hull M, Webster P, Male P, Goud B, Mellman I. The small GTP-binding protein rab4 controls an early sorting event on the endocytic pathway. Cell 1992;70:729-740.
4. Bucci C, Parton RG, Mather IH, Stunnenberg H, Simons K, Hoflack B, Zerial M. The small GTPase rab5 functions as a regulatory factor in the early endocytic pathway. Cell 1992;70:715-728.
5. Martinez O, Schmidt A, Salamero J, Hoflack B, Roa M, Goud B. The small GTP-binding protein rab6 functions in intra-Golgi transport. J Cell Biol 1994;127:1575-1588.
6. Bucci C, Thomsen P, Nicoziani P, McCarthy J, van Deurs B. Rab7: a key to lysosome biogenesis. Mol Biol Cell 2000;11:467-480.
7. Yang M, Chen T, Han C, Li N, Wan T, Cao X. Rab7b, a novel lysosome-associated small GTPase, is involved in monocytic differentiation of human acute promyelocytic leukemia cells. Biochem Biophys Res Commun 2004;318:792-799.
8. Chen YT, Holcomb C, Moore HP. Expression and localization of two low molecular weight GTP-binding proteins, Rab8 and Rab10, by epitope tag. Proc Natl Acad Sci U S A 1993;90:6508-6512.
9. Lombardi D, Soldati T, Riederer MA, Goda Y, Zerial M, Pfeffer SR. Rab9 functions in transport between late endosomes and the trans Golgi network. EMBO J 1993;12:677-682.
10. Cardoso CM, Jordao L, Vieira OV. Rab10 regulates phagosome maturation and its overexpression rescues *Mycobacterium*-containing phagosomes maturation. Traffic 2010;11:221-235.
11. Cox D, Lee DJ, Dale BM, Calafat J, Greenberg S. A Rab11-containing rapidly recycling compartment in macrophages that promotes phagocytosis. Proc Natl Acad Sci U S A 2000;97:680-685.
12. Nokes RL, Fields IC, Collins RN, Folsch H. Rab13 regulates membrane trafficking between TGN and recycling endosomes in polarized epithelial cells. J Cell Biol 2008;182:845-853.
13. Junutula JR, De Maziere AM, Peden AA, Ervin KE, Advani RJ, van Dijk SM, Klumperman J, Scheller RH. Rab14 is involved in membrane trafficking between the Golgi complex and endosomes. Mol Biol Cell 2004;15:2218-2229.
14. Pavlos NJ, Xu J, Riedel D, Yeoh JS, Teitelbaum SL, Papadimitriou JM, Jahn R, Ross FP, Zheng MH. Rab3D regulates a novel vesicular trafficking pathway that is required for osteoclastic bone resorption. Mol Cell Biol 2005;25:5253-5269.
15. Dejgaard SY, Murshid A, Erman A, Kizilay O, Verbich D, Lodge R, Dejgaard K, Ly-Hartig TB, Pepperkok R, Simpson JC, Presley JF. Rab18 and Rab43 have key roles in ER-Golgi trafficking. J Cell Sci 2008;121:2768-2781.
16. Das Sarma J, Kaplan BE, Willemsen D, Koval M. Identification of rab20 as a potential regulator of connexin 43 trafficking. Cell Commun Adhes 2008;15:65-74.
17. Pellinen T, Arjonen A, Vuoriluoto K, Kallio K, Fransen JA, Ivaska J. Small GTPase Rab21 regulates cell adhesion and controls endosomal traffic of beta1-integrins. J Cell Biol 2006;173:767-780.
18. Kauppi M, Simonsen A, Bremnes B, Vieira A, Callaghan J, Stenmark H, Olkkonen VM. The small GTPase Rab22 interacts with EEA1 and controls endosomal membrane trafficking. J Cell Sci 2002;115:899-911.
19. Ng EL, Wang Y, Tang BL. Rab22B's role in trans-Golgi network membrane dynamics. Biochem Biophys Res Commun 2007;361:751-757.
20. Evans TM, Ferguson C, Wainwright BJ, Parton RG, Wicking C. Rab23, a negative regulator of hedgehog signaling, localizes to the plasma membrane and the endocytic pathway. Traffic 2003;4:869-884.
21. Strom M, Hume AN, Tarafder AK, Barkagianni E, Seabra MC. A family of Rab27-binding proteins. Melanophilin links Rab27a and myosin Va function in melanosome transport. J Biol Chem 2002;277:25423-25430.
22. Wasmeier C, Romao M, Plowright L, Bennett DC, Raposo G, Seabra MC. Rab38 and Rab32 control post-Golgi trafficking of melanogenic enzymes. J Cell Biol 2006;175:271-281.
23. Wang T, Hong W. Interorganellar regulation of lysosome positioning by the Golgi apparatus through Rab34 interaction with Rab-interacting lysosomal protein. Mol Biol Cell 2002;13:4317-4332.
24. Kouranti I, Sachse M, Arouche N, Goud B, Echard A. Rab35 regulates an endocytic recycling pathway essential for the terminal steps of cytokinesis. Curr Biol 2006;16:1719-1725.
25. Masuda ES, Luo Y, Young C, Shen M, Rossi AB, Huang BC, Yu S, Bennett MK, Payan DG, Scheller RH. Rab37 is a novel mast cell specific GTPase localized to secretory granules. FEBS Lett 2000;470:61-64.

Table S2 Primer list for construction of plasmid of EGFP-fused Rab GTPases

Rab GTPase	Primer forward	Primer reverse
Rab1	CAGATCTatgtccagcatgaatcccgaatatg	CGGTACCttagcagcaacctccacctg
Rab1b	CAGATCTatgaaccccgaatatgactacctgtttaag	CGAATTCtagcagcagccaccgctagcaggct
Rab2	CAGATCTatggcgtacgcctatctcttcaag	CCCGAATTCtcaacagcagccgccccca
Rab2b	CAGATCTatgacttatgcttatctcttcaagtatatc	CGAATTCtcagcagcagccagagttggaccctatgtc
Rab3	CCTCGAGCTatggcatccgccacagactcgc	CGAATTCtcagcaggcgcagtcctggt
Rab3b	CCTCGAGCTatggcttcagtgacagatggtaaaactgg	CGAATTCCtagcatgagcagttctgctgcagcagc
Rab4	CAGATCTatgtcgcagacggccatgtccgaaacc	CGAATTCtaacaaccacactcctgagcgttcg
Rab4b	CAGATCTatggctgagacctacgacttcctct	CGAATTCagcagccacacggctgaggggcc
Rab5	CAGATCTatggctagtcgaggcgcaacaagac	CGAATTCttagttactacaacactgattcctgg
Rab5b	CCTCGAGCTatgactagcagaagcacagctaggcc	CGAATTCagttgctacaacactggctcttg
Rab6	CCTCGAGCTatgtccacgggcggagactt	CGAATTCttagcaggaacagcctccttcac
Rab6b	CAGATCTatgtccgcagggggagattttggga	CGAATTCttagcaggagcagccgccctcgctggc
Rab7b	CCTCGAGCTatgaatccccggaagaaggt	CGAATTCagcagcatctgctccttgactggtctgg
Rab8	CAGATCTatggcgaagacctacgattacctg	CGAATTCtcacagaagaacacatcggaaaaagctg
Rab8b	CAGATCTatggcgaagacgtacgattatctcttcaag	CGAATTCaaagtagcgagcaacgaaagaaactggtc
Rab9	CAGATCTatggcaggaaaatcatcacttttaaag	CGGTACCtcaacagcaagatgagctaggc
Rab9b	CCTCGAGCTatgagtgggaaatccctgctcttaaag	CGAATTCttaacagcacgaagaccctgctttggagc
Rab10	CAGATCTatggcgaagaagacgtacgacctg	CGAATTCtcagcagcatttgctcttccagc
Rab11	CAGATCTatgggcacccgcgacgacgag	CGAATTCttagatgttctgacagcactgcacc
Rab11b	CCTCGAGCTatggggacccgggacgacgagtacg	CGAATTCacaggttctggcagcactgcagctt
Rab13	CAGATCTatggccaaagcctacgaccac	CGAATTCtcagcccagggagcacttgttg
Rab14	CAGATCTatggcaactgcaccatacaactactc	CGAATTCctagcagccacagccttctc
Rab16	CCTCGAGCTatggcatcagctggagacacc	CGAATTCctagcagctgcagctgctgg
Rab18	CAGATCTatggacgaggacgtgctaacca	CGAATTCttataacacagagcaataaccaccacag
Rab20	CCTCGAGCTatgaggaagcccgacagcaag	CGAATTCtcaggcacaacacccagatctg
Rab21	CAGATCTccgggaagcgacgggatggc	CGAATTCttatccagaagaacagcaccctcc
Rab22a	CAGATCTatggcgctgagggagctcaa	CGGTACCtcagcagcagctccgctttg
Rab22b	CAGATCTatgatggcgatacgggagctcaaagtg	CGAATTCaacagcaccggcggctggcttgc
Rab23	CCTCGAGCTatgttggaggaagatatggaagtcgc	CAAGCttagggtatgctacagctgctaaaagg
Rab24	CAGATCTatgagcgggcagcgcgtgga	CGAATTCtcagtgatgacaacagctgtagaag
Rab27	CAGATCTatgtctgatggagattatgattacctc	CGAATTCtcaacagccacatgccccctttctc
Rab28	CAGATCTatgtcggactctgaggaggag	CGAATTCtcactgaactgcacacatagagcttc
Rab29	CAGATCTatgggcagccgcgaccacct	CGAATTCctagcagcaggaccagctgg
Rab30	CCTCGAGCTatgagtatggaagattatgatttcctgttc	CGGTACCttagttgaaattacaacaagtcaaatagctg
Rab32	CCAGATCTatggcgggcggaggagccgg	CGAATTCtcagcaacactgggatttgttctctg
Rab34	CCTCGAGCTatgaacattctggcacccgtgc	CGGTACCtcatgggcaacatgtgggcttc
Rab35	CCTCGAGCTatggcccgggactacgacca	CGAATTCttagcagcagcgtttctttcgtttactg
Rab37	CCTCGAGCTatgacgggcacgccaggcgccgttg	CGAATTCacatgaaggagcagcagctggag
Rab38	CAGATCTatgcaggccccgcacaagga	CGAATTCctaggatttggcacagccagag
Rab39	CAGATCTatggagaccatctggatctaccag	CGAATTCtcagcagaagcattctttcctggg
Rab43	CAAGCTTCGcggcccttcggcttcttctag	CGAATTCggctctggagggctgggctt

Table S3 Primer list for site-directed mutagenesis

Rab GTPase	dominant negative	constitutive acitive	dominant negative-F	dominant negative-R	constitutive active-F	constitutive active-R
Rab5	S34N	Q79L	agagtccgctgttggcaaaAATagcctagtgcttcgtttt	aaaacgaagcactaggctATTtttgccaacagcggactct	gaaatatgggatacagctggtcTagaacgataccatagcctag	ctaggctatggtatcgttctAgaccagctgtatcccatatttc
Rab7b	T22N	Q67L	gccattggtgtgggaaagaActccctccctcaccaatatg	catattggtgagggagggagTtctttcccacaccaatggc	gatctgggacacgggcggtcTggagcggttccgctccatg	catggagcggaaccgctccAgaccgcccgtgtcccagatc
Rab8	T22N	Q67L	gactcgggggtggggaagaActgtgtcctgttccgcttc	gaagcggaacaggacacagTtcttccccacccccgagtc	gatatgggacacagccggtcTggaacggtttcggacgatc	gatcgtccgaaaccgttccAgaccggctgtgtcccatatc
Rab8b	T22N	Q67L	ctcgggggtaggcaagaActgcctcctgttccgcttctc	gagaagcggaacaggaggcagTtcttgcctaccccgag	gatatgggacacagcgggtcTggaaagattccgaacaatc	gattgttcggaatctttccAgacccgctgtgtcccatatc
Rab9	S21N	Q66L	gatggtggagttgggaagaAttcacttatgaacagatatg	catatctgttcataagtgaaTtcttcccaactccaccatc	gggacacggcaggtcTggagcgattccgaagcctgaggac	gtcctcaggcttcggaatcgctccAgacctgccgtgtccc
Rab9b	S21N	Q66L	gatggtggagttgggaaaaACtcgcttatgaaccgttacg	cgtaacggttcataagcgaGTttttcccaactccaccatc	ctgggacactgcagggcTggaacgtttcaagagccttag	ctaaggctcttgaaacgttccAgccctgcagtgtcccag
Rab11	S25N	Q70L	gattctggtgttggaaagaAtaatctcctgtctcgatttac	gtaaatcgagacaggagattaTtctttccaacaccagaatc	gatatgggacacagcagggcTGgagcgatatcgagctataac	gttatagctcgatatcgctcCAgccctgctgtgtcccatatc
Rab11b	S25N	Q70L	gactcaggcgtgggcaagaAcaacctgctgtcgcgcttc	gaagcgcgacagcaggttgTtcttgcccacgcctgagtc	gatctgggacaccgctggccTggagcgctaccgccgcatc	gatgcggcggtagcgctccAggccagcggtgtcccagatc
Rab13	T22N	Q67L	gactcgggggtgggcaagaACtgtctgatcattcgctttg	caaagcgaatgatcagacaGTtcttgcccacccccgagtc	gtctgggacacggctggccTagagcggttcaagacaataac	gttattgtcttgaaccgctctAggccagccgtgtcccagac
Rab14	S25N	Q70L	gacatgggagtaggaaaaAAttgcttgcttcatcaatttac	gtaaattgatgaagcaagcaaTTttttcctactcccatgtc	gatttgggatacggcaggacTggagcgatttagggctgttac	gtaacagccctaaatcgctccAgtcctgccgtatcccaaatc
Rab20	T19N	R59L	catgaacgtggggaagaATtcgctgctgcagcggtatatg	catataccgctgcagcagcgaATtcttccccacgttcatg	gggacaccgcagggcTggagcagttccacggcctgggatc	gatcccaggccgtggaactgctccAgccctgcggtgtccc
Rab22a	S19N	Q64L	caggtgtaggtaaaAACagtattgtgtggcggtttgtgg	ccacaaaccgccacacaatactGTTtttacctacacctg	ctgggatacagctggacTCgaacgatttcgtgccttag	ctaaggcacgaaatcgttcGAgtccagctgtatcccag
Rab22b	S20N	Q65L	gacactggggttgggaaaAACagcatcgtgtgtcgatttgtc	gacaaatcgacacacgatgctGTTtttcccaaccccagtgtc	catctgggacactgctggtcTTgaacggtttcattcattgg	ccaatgaatgaaaccgttcAAgaccagcagtgtcccagatg
Rab23	S23N	Q68L	gaatggagcagttggaaaaAATagtatgattcagcgatattg	caatatcgctgaatcatactATTttttccaactgctccattc	gttatgggacactgcaggtcTTgaggaatttgatgcaattac	gtaattgcatcaaattcctcAAgacctgcagtgtcccataac
Rab27	T23N	Q78L	ctctggtgtagggaagaAcagtgtactttaccaatatac	gtatattggtaaagtacactgTtcttccctacaccagag	gttatgggacacagcagggcTggagaggtttcgtagcttaac	gttaagctacgaaacctctccAgccctgctgtgtcccataac
Rab32	T39N	Q85L	gagcttggcgtgggcaagaAcagcatcatcaagcgctacg	cgtagcgcttgatgatgctgTtcttgcccacgccaagctc	gctgtgggacatcgcgggcTggagcgatttggcaacatg	catgttgccaaatcgctccAgccccgcgatgtcccacagc
Rab34	T66N	Q111L	gacctgtcggtggggaagaAttgcctcattaataggttc	gaacctattaatgaggcaaTtcttccccaccgacaggtc	ctttgggataccgctgggcTggagaggttcaaatgcattg	caatgcatttgaacctctccAgcccagcggtatcccaaag
Rab37	T43N	Q89L	gagacacaggcgtcggcaaaaACtgtttcctgatccaattc	gaattggatcaggaaacaGTttttgccgacgcctgtgtctc	gatctgggacaccgctgggcTggaacggttccgaagcgtc	gacgcttcggaaccgttccAgcccagcggtgtcccagatc
Rab38	T23N	Q69L	gacctgggcgtggggaagaAcagtatcatcaagcgctacg	cgtagcgcttgatgatactgTtcttccccacgcccaggtc	ctgggatatcgcaggtcTCgaaagatttggaaacatgac	gtcatgtttccaaatctttcGAgacctgcgatatcccag
Rab39	S22N	Q72L	gactccaccgtgggcaagAActgcctcctgcaccgcttc	gaagcggtgcaggaggcagTTcttgcccacggtggagtc	ctctgggacacggcgggacTggagcggttcagatcaataac	gttattgatctgaaccgctccAgtcccgccgtgtcccagag
Rab43	T32N	Q77L	cgacgcaagcgtgggcaagaACtgcgtggtgcagcgcttc	gaagcgctgcaccacgcaGTtcttgcccacgcttgcgtcg	gatctgggacacggccggccTggagcggttccgcaccatc	gatggtgcggaaccgctccAggccggccgtgtcccagatc

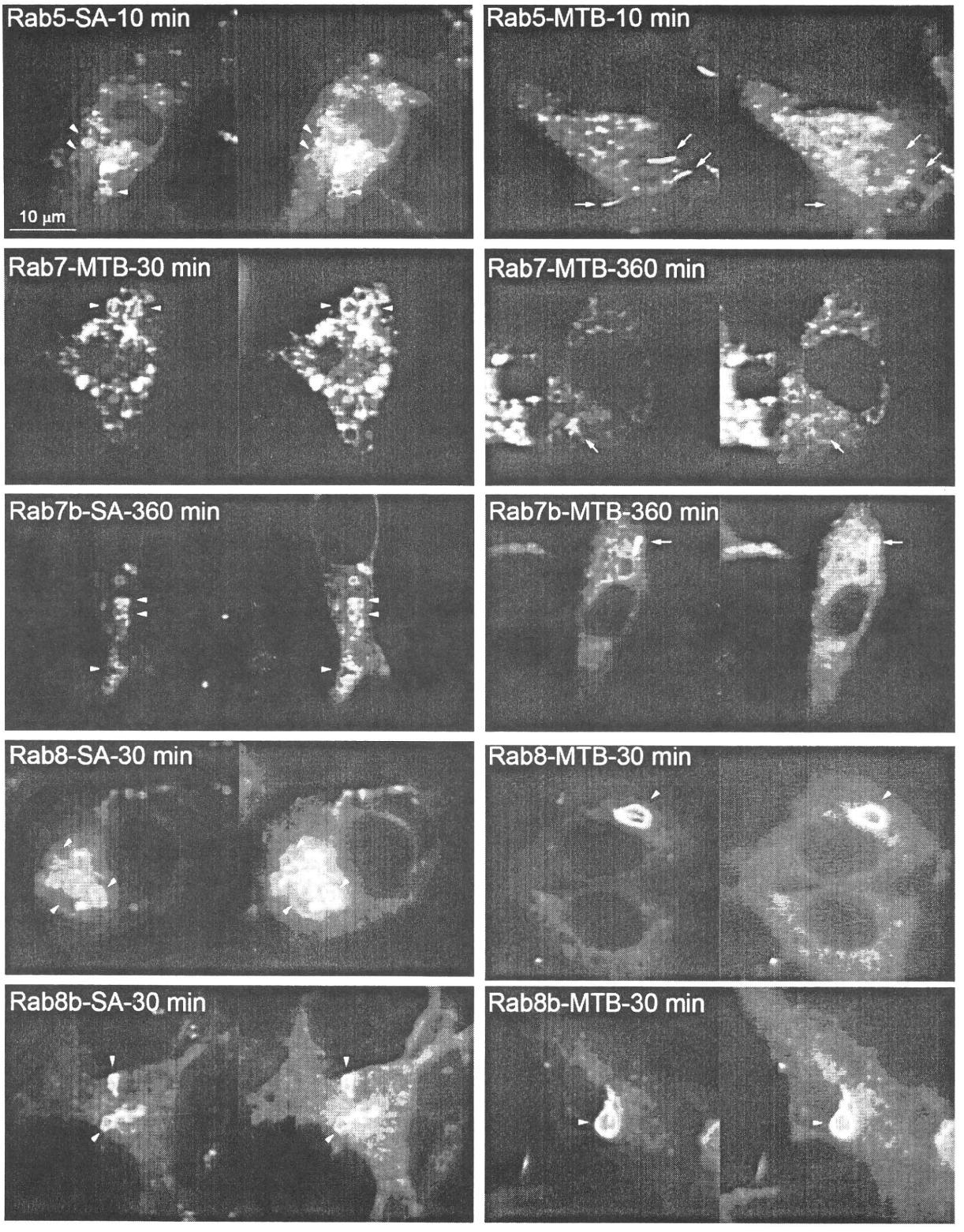
Rab5-SA-10 min
10 μm
Rab5-MTB-10 min
Rab7-MTB-30 min
Rab7-MTB-360 min
Rab7b-SA-360 min
Rab7b-MTB-360 min
Rab8-SA-30 min
Rab8-MTB-30 min
Rab8b-SA-30 min
Rab8b-MTB-30 min

Figure S1-1

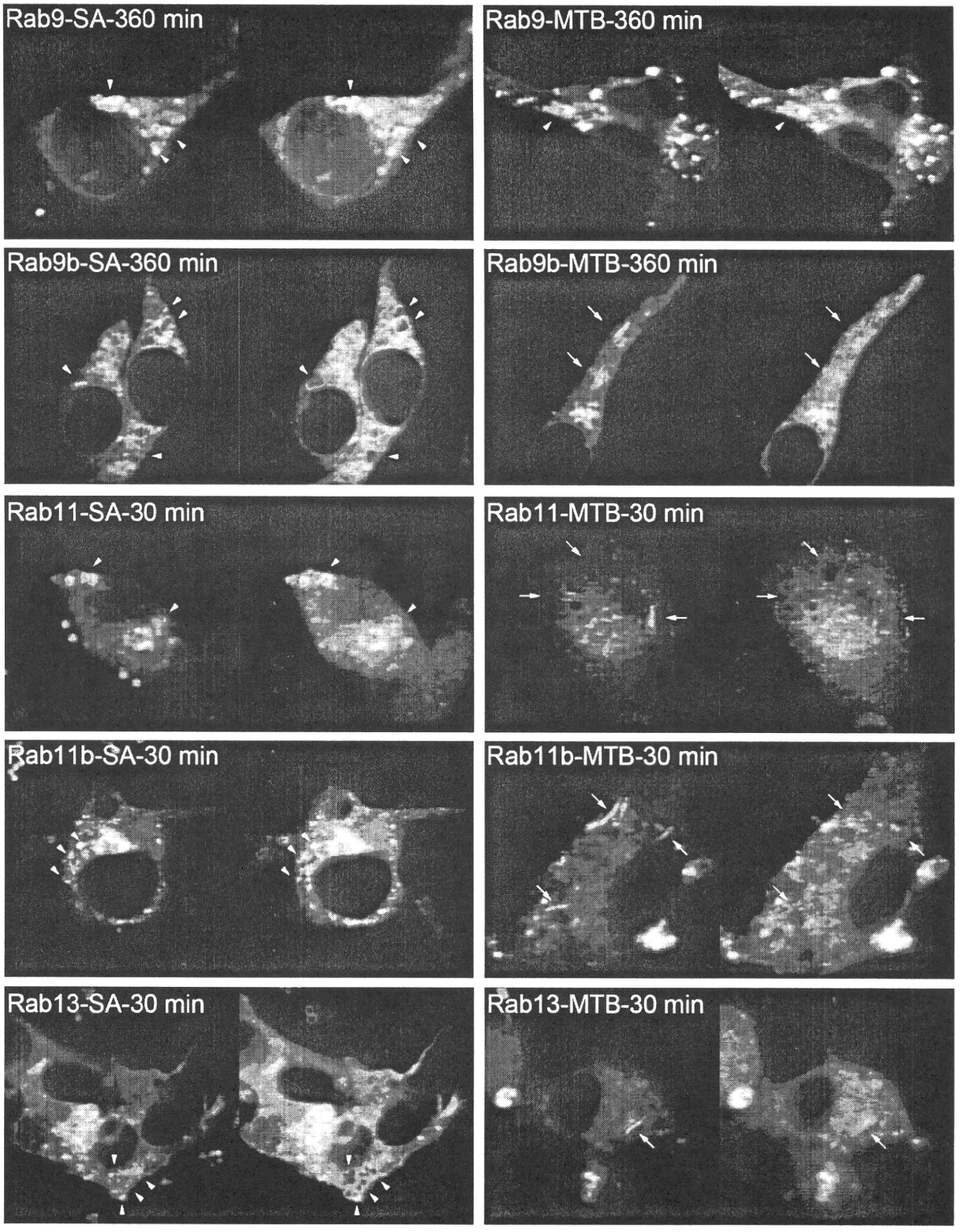
Rab9-SA-360 min
Rab9-MTB-360 min
Rab9b-SA-360 min
Rab9b-MTB-360 min
Rab11-SA-30 min
Rab11-MTB-30 min
Rab11b-SA-30 min
Rab11b-MTB-30 min
Rab13-SA-30 min
Rab13-MTB-30 min

Figure S1-2

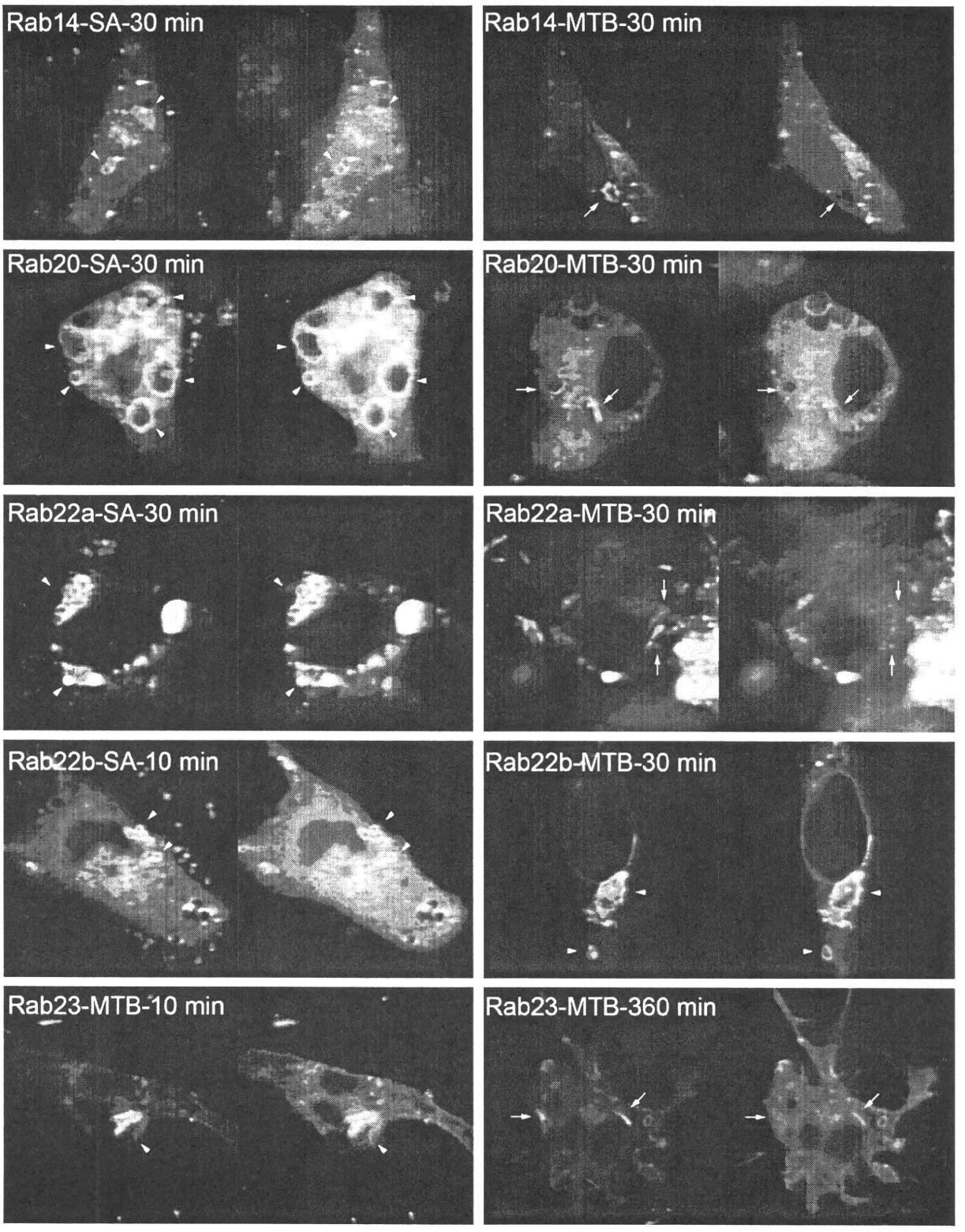
Rab14-SA-30 min
Rab14-MTB-30 min
Rab20-SA-30 min
Rab20-MTB-30 min
Rab22a-SA-30 min
Rab22a-MTB-30 min
Rab22b-SA-10 min
Rab22b-MTB-30 min
Rab23-MTB-10 min
Rab23-MTB-360 min

Figure S1-3

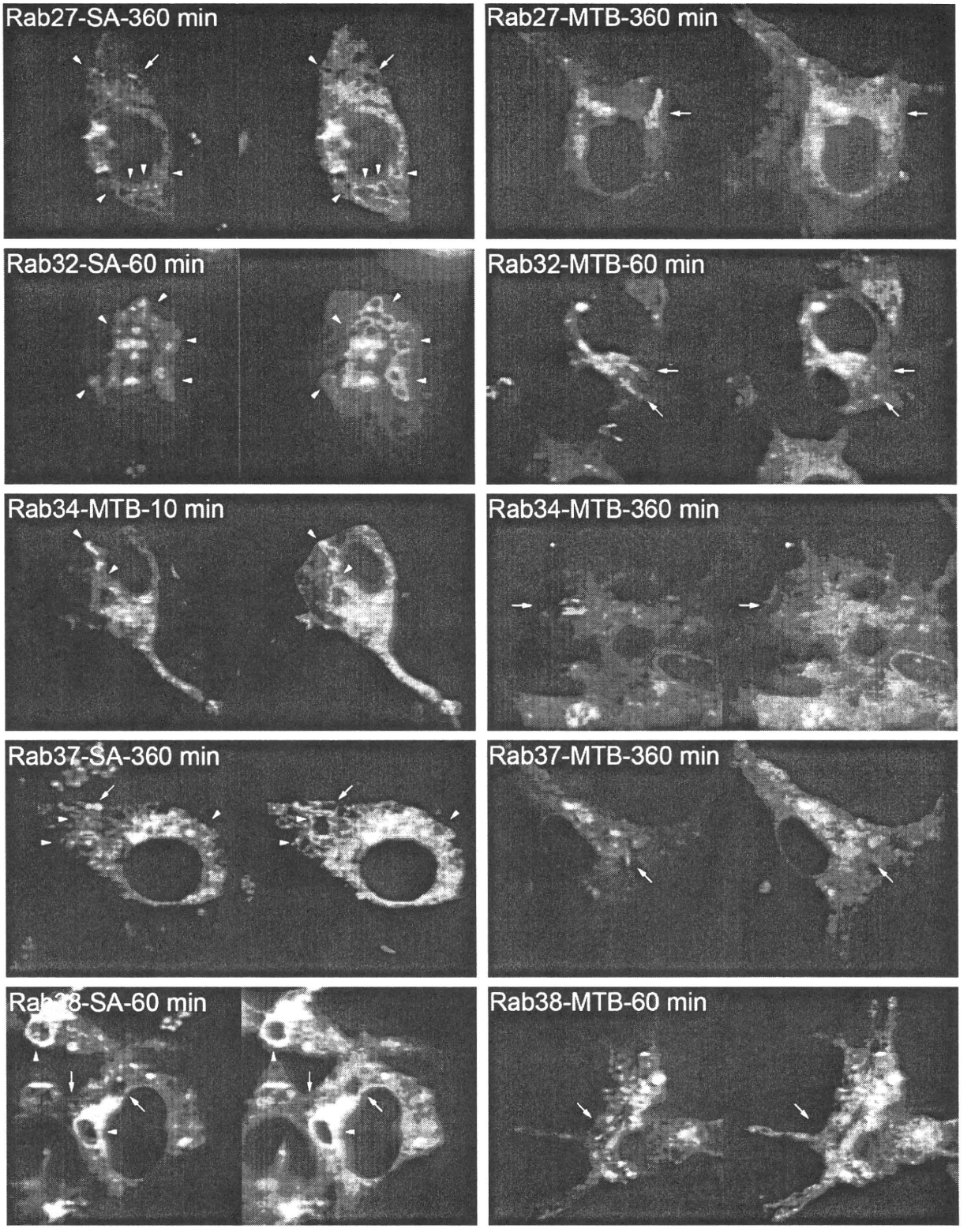
Rab27-SA-360 min
Rab27-MTB-360 min
Rab32-SA-60 min
Rab32-MTB-60 min
Rab34-MTB-10 min
Rab34-MTB-360 min
Rab37-SA-360 min
Rab37-MTB-360 min
Rab38-SA-60 min
Rab38-MTB-60 min

Figure S1-4

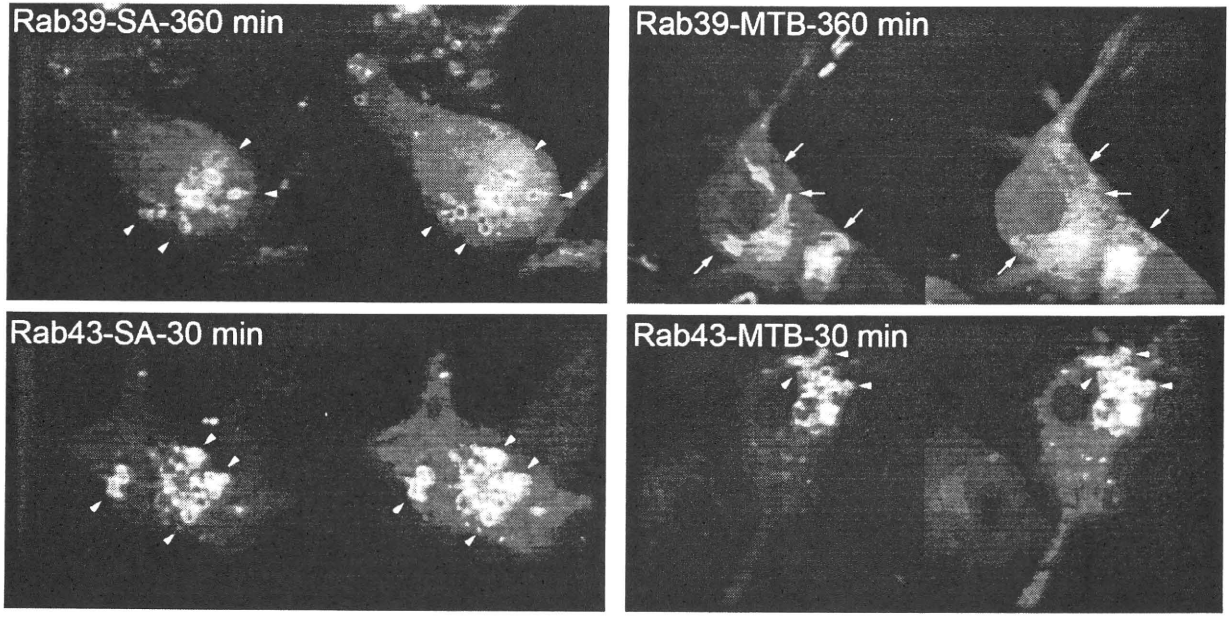
Rab39-SA-360 min
Rab39-MTB-360 min
Rab43-SA-30 min
Rab43-MTB-30 min

Figure S1-5

(A)

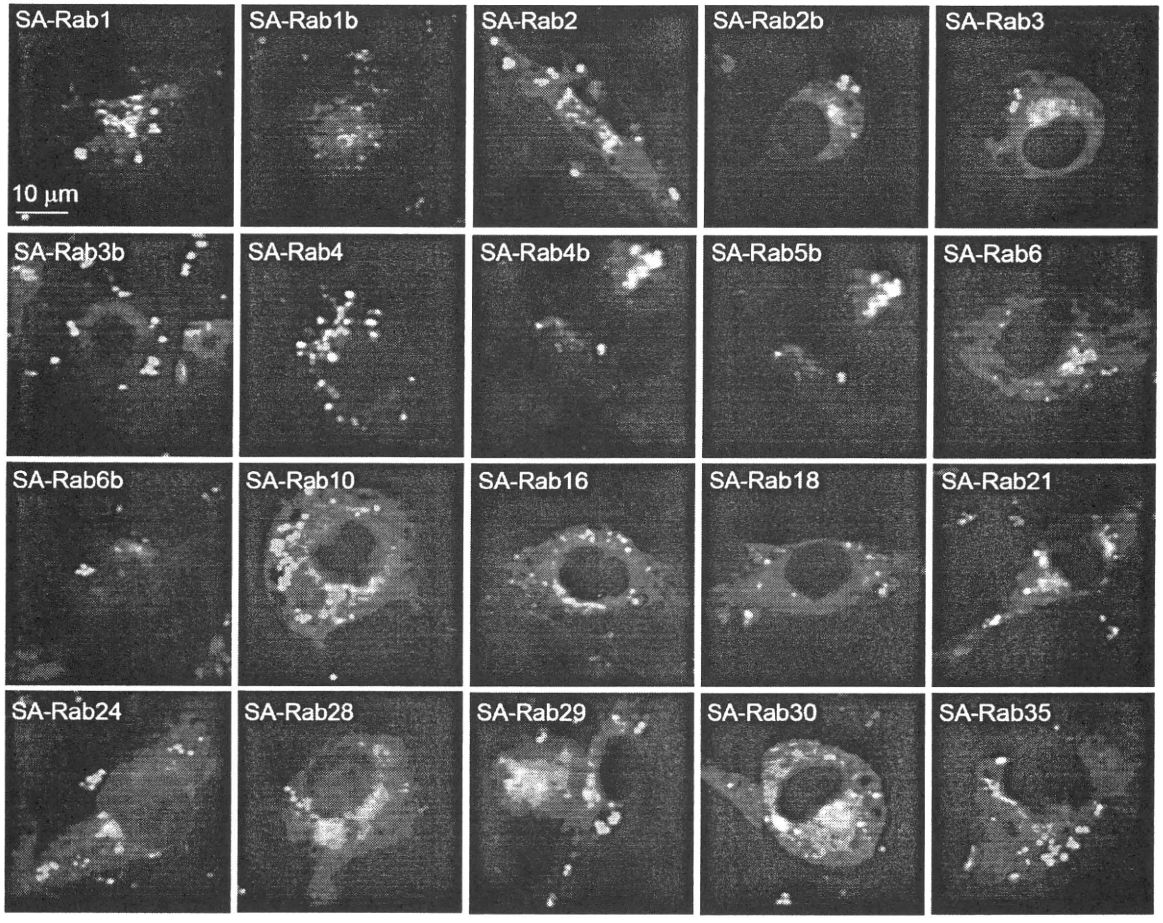
SA-Rab1
SA-Rab1b
SA-Rab2
SA-Rab2b
SA-Rab3
10 μm
SA-Rab3b
SA-Rab4
SA-Rab4b
SA-Rab5b
SA-Rab6
SA-Rab6b
SA-Rab10
SA-Rab16
SA-Rab18
SA-Rab21
SA-Rab24
SA-Rab28
SA-Rab29
SA-Rab30
SA-Rab35

Figure S2A

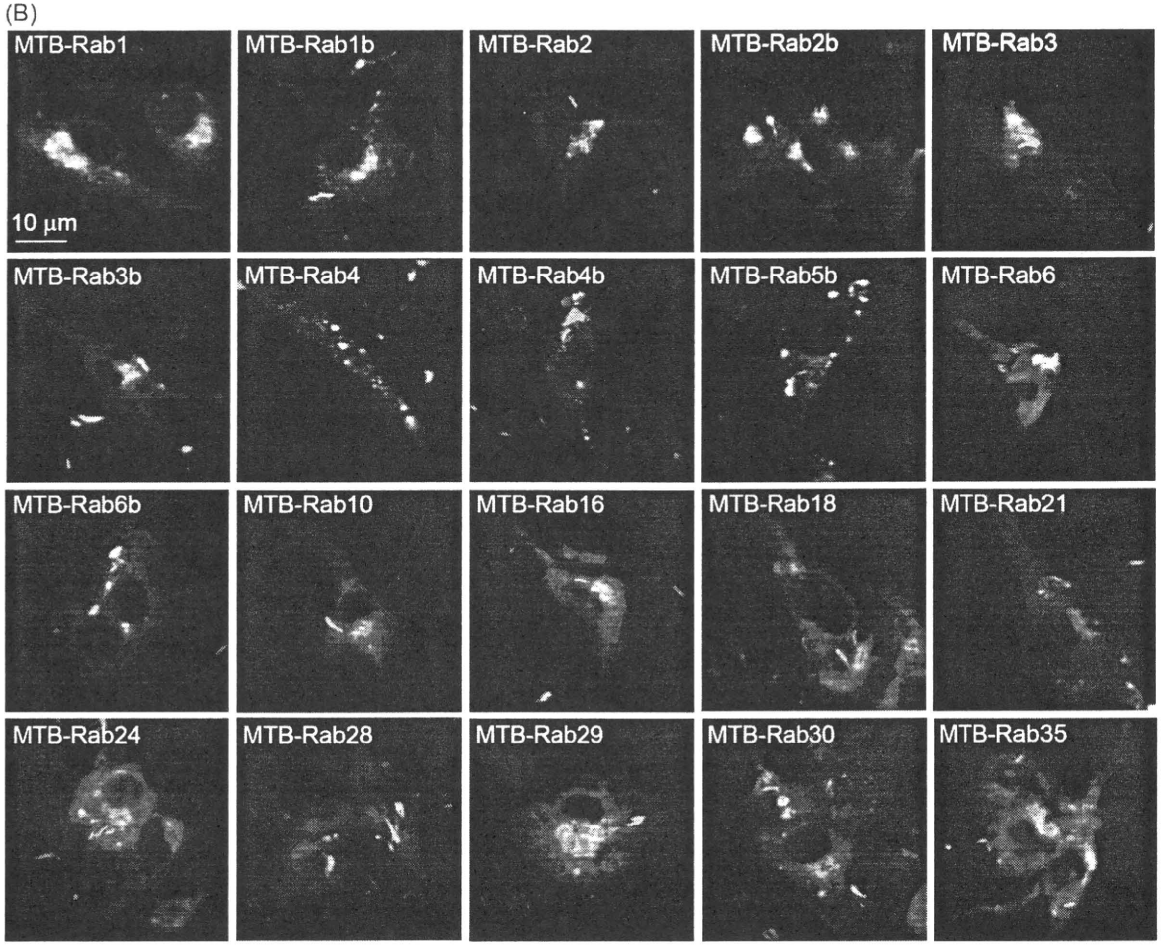
(B)
MTB-Rab1
MTB-Rab1b
MTB-Rab2
MTB-Rab2b
MTB-Rab3
10 μm
MTB-Rab3b
MTB-Rab4
MTB-Rab4b
MTB-Rab5b
MTB-Rab6
MTB-Rab6b
MTB-Rab10
MTB-Rab16
MTB-Rab18
MTB-Rab21
MTB-Rab24
MTB-Rab28
MTB-Rab29
MTB-Rab30
MTB-Rab35

Figure S2B

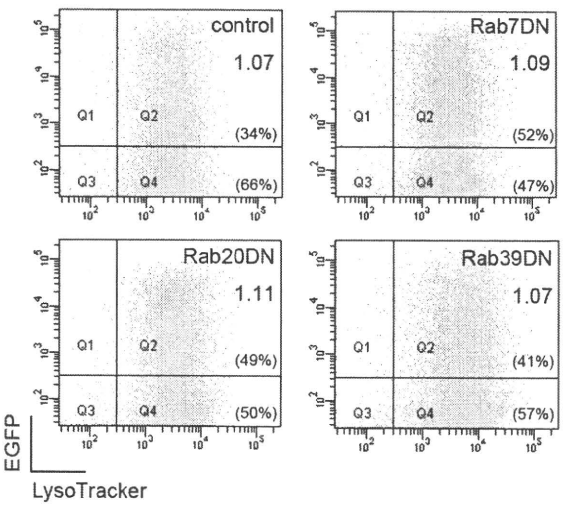
control
1.07
Q1
Q2
(34%)
Q3
Q4
(66%)
Rab7DN
1.09
Q1
Q2
(52%)
Q3
Q4
(47%)
Rab20DN
1.11
Q1
Q2
(49%)
Q3
Q4
(50%)
Rab39DN
1.07
Q1
Q2
(41%)
Q3
Q4
(57%)
EGFP
LysoTracker

Figure S3

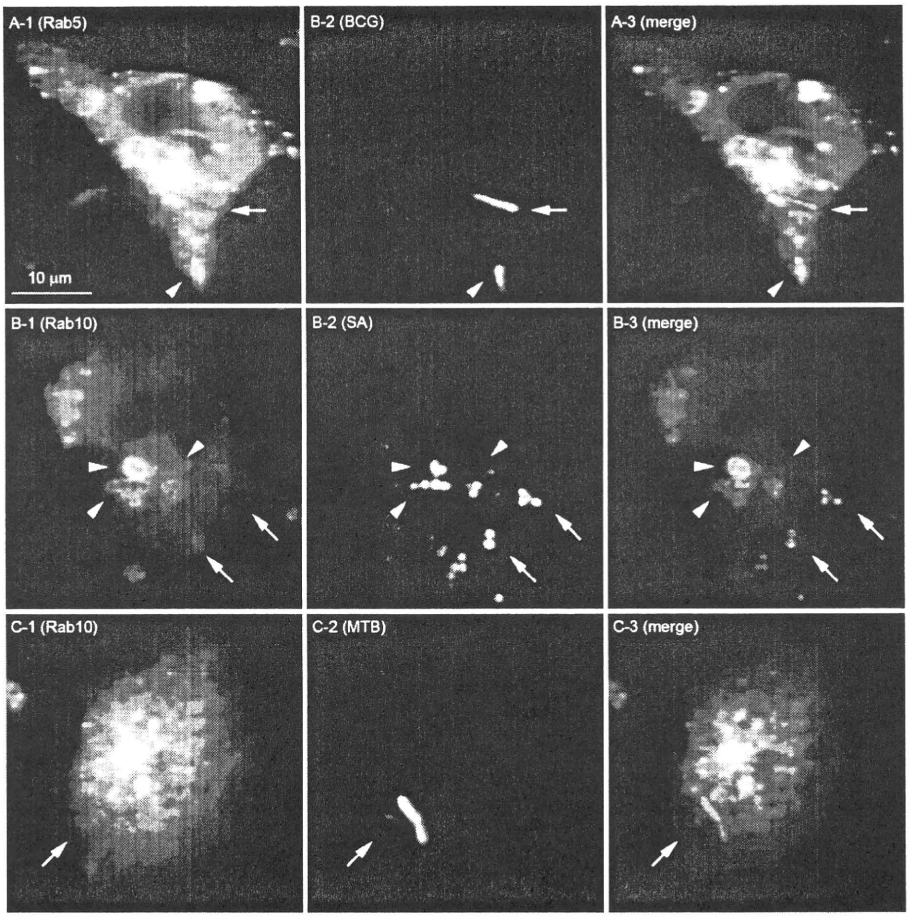
A-1 (Rab5)
B-2 (BCG)
A-3 (merge)
10 μm
B-1 (Rab10)
B-2 (SA)
B-3 (merge)
C-1 (Rab10)
C-2 (MTB)
C-3 (merge)

Figure S4

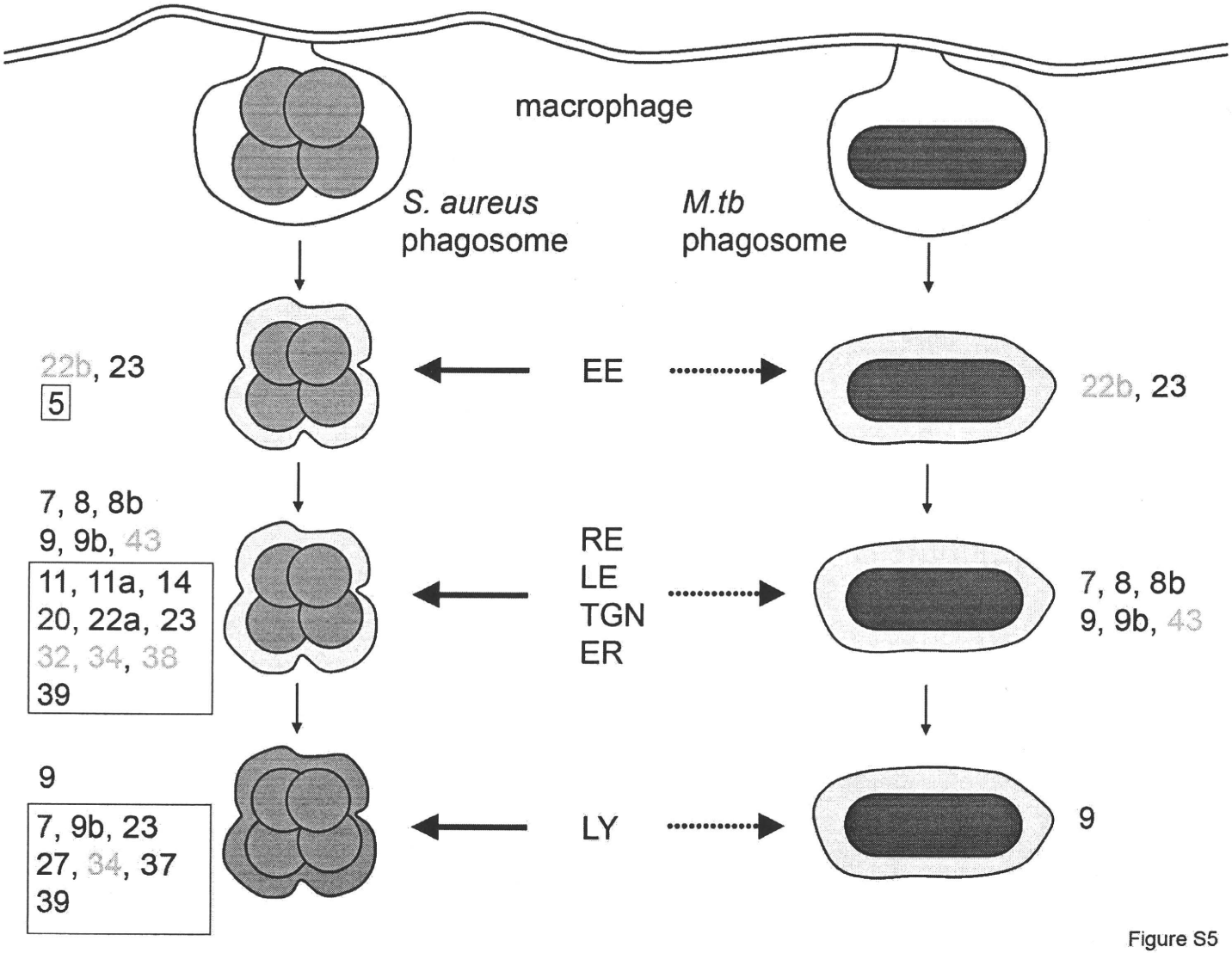
macrophage
S. aureus phagosome
M.tb phagosome
22b, 23
5
EE
22b, 23
7, 8, 8b
9, 9b, 43
11, 11a, 14
20, 22a, 23
32, 34, 38
39
RE
LE
TGN
ER
7, 8, 8b
9, 9b, 43
9
7, 9b, 23
27, 34, 37
39
LY
9

Figure S5

FEMS IMMUNOLOGY & MEDICAL MICROBIOLOGY

RESEARCH ARTICLE

A novel vaccine strategy to induce mycobacterial antigen-specific Th1 responses by utilizing the C-terminal domain of heat shock protein 70

Tomohiro Uto[1,2], Kunio Tsujimura[1], Masato Uchijima[1], Shintaro Seto[1], Toshi Nagata[1,3], Takafumi Suda[2], Kingo Chida[2], Hirotoshi Nakamura[2] & Yukio Koide[1]

[1]Department of Infectious Diseases, Hamamatsu University School of Medicine, Hamamatsu, Japan; [2]Department of Internal Medicine, Hamamatsu University School of Medicine, Hamamatsu, Japan; and [3]Department of Health Science, Hamamatsu University School of Medicine, Hamamatsu, Japan

Correspondence: Yukio Koide, Department of Infectious Diseases, Hamamatsu University School of Medicine, 1-20-1 Handa-yama, Higashi-ku, Hamamatsu 431-3192, Japan. Tel.: +81 53 435 2101; fax: +81 53 435 2335; e-mail: koidelb@hama-med.ac.jp

Received 30 June 2010; revised 26 October 2010; accepted 19 November 2010.

DOI:10.1111/j.1574-695X.2010.00762.x

Editor: Willem van Eden

Keywords
Mycobacterium tuberculosis; heat shock protein; DNA vaccine; IFN-γ.

Abstract

Heat shock protein 70 (HSP70) is a member of a highly conserved superfamily of intracellular chaperones called stress proteins that can activate innate and adaptive immune responses. We evaluated the effect of a fusion DNA vaccine that encoded mycobacterial HSP70 and MPT51, a major secreted protein of *Mycobacterium tuberculosis*. Spleen cells from mice immunized with fusion DNA of full-length HSP70 and MPT51 produced a higher amount of interferon-γ (IFN-γ) in response to the CD4+, but not the CD8+ T-cell epitope peptide on MPT51 than those from mice immunized with MPT51 DNA. Furthermore, because HSP70 comprises the N-terminal ATPase domain and the C-terminal peptide-binding domain, we attempted to identify the domain responsible for its enhancing effect. The fusion DNA vaccine that encoded the C-terminal domain of HSP70 and MPT51 induced a higher MPT51-specific IFN-γ production by CD4+ T cells than the vaccine that encoded MPT51 alone, whereas that with the N-terminal domain did not. Similar results were obtained by immunization with the fusion proteins. These results suggest that the DNA vaccine that encodes a chimeric antigen molecule fused with mycobacterial HSP70, especially with its C-terminal domain, can induce a stronger antigen-specific T-helper cell type 1 response than antigen DNA alone.

Introduction

Tuberculosis is a major cause of death worldwide. There were an estimated 9.4 million incident and 11.1 million prevalent cases of tuberculosis, and 1.8 million people died of tuberculosis, in 2008 (World Health Organization, 2009). *Mycobacterium bovis* Bacillus Calmette–Guerin (BCG) is the only available vaccine against tuberculosis, but it has been reported to show variable protective efficacy (Colditz *et al.*, 1994). Although BCG can protect against tuberculosis in childhood, its efficacy in adults varies, especially in endemic countries (Sterne *et al.*, 1998; Kaufmann, 2004; Andersen, 2007). It is also known to represent a risk for immunocompromised patients. In addition, the emergence of multidrug-resistant strains of *Mycobacterium tuberculosis* has lent urgency to the search for novel therapeutic agents and the development of more effective vaccines capable of protecting adults (Kaufmann, 2000).

MPT51 is a major secreted protein of *M. tuberculosis*, which has a molecular weight of 27 kDa and a primary structure that is similar to the components of the antigen 85 complex (Nagai *et al.*, 1991; Ohara *et al.*, 1995, 1997). We demonstrated previously that MPT51 induces T-cell-mediated immune responses and protective immunity against challenge with *M. tuberculosis* in mice (Miki *et al.*, 2004), and have identified one CD8+ and two CD4+ T-cell epitopes that are presented by H2-D^d and H2-A^b, respectively (Suzuki *et al.*, 2004). MPT51 is recognized by T cells from patients with active tuberculosis and is also considered to be immunogenic in humans (de Araujo-Filho *et al.*, 2008).

Heat shock protein70 (HSP70) is a member of a highly conserved superfamily of intracellular chaperones called

stress proteins (Gething *et al.*, 1995). In addition, HSP70 appears to play important roles in the innate and adaptive immune responses, such as receptor-mediated antigen internalization by sentinel antigen-presenting cells (APCs), stimulation of production of various cytokines, and maturation of dendritic cells (DCs) (Suto & Srivastava, 1995; Basu *et al.*, 2000; Binder *et al.*, 2000; Castellino *et al.*, 2000; Singh-Jasuja *et al.*, 2000). Collectively, the ability of HSP70 to bind antigenic peptides and deliver them to APCs profoundly contributes to the generation of antigen-specific T-cell responses.

In this study, we compared the effect of a DNA vaccine that encoded a fusion protein that consisted of MPT51, a protective antigen against *M. tuberculosis* (Miki *et al.*, 2004), and *M. tuberculosis* HSP70 on the induction of MPT51-specific T-cell responses, with that of MPT51 DNA alone. After showing superior MPT51-specific T-cell induction by the fusion molecule, we attempted to establish the domain of HSP70 that was responsible for this enhancing effect.

Materials and methods

Construction of fusion genes for DNA vaccines

Mycobacterium tuberculosis HSP70 gene was cloned by PCR from genomic DNA of the H37Rv strain. The primers used for PCR were as follows:

HSP70F (full-length HSP70: residues 1–625)

5′-TATGAATTCACCATGGCTCGTGCGGTCGGG-3′ (forward)

5′-AATGGTACCCTTGGCCTCCCGGCCGT-3′ (reverse)

HSP70N (N-terminal domain of HSP70: residues 1–360)

5′-TATGAATTCACCATGGCTCGTGCGGTCGGG-3′ (forward)

5′-AATGGTACCCACCTCGCCCTTGAGGA-3′ (reverse)

HSP70C (C-terminal domain of HSP70: residues 354–625)

5′-TATGAATTCACCATGGCGTCCTCAAGGGC-3′ (forward)

5′-AATGGTACCCTTGGCCTCCCGGCCGT-3′ (reverse)

Forward and reverse primers contained EcoRI and KpnI restriction sites (underlined), respectively. PCR products were purified and cloned into the EcoRI/KpnI sites of the pCI vector (Promega, Madison, WI) that contained MPT51 DNA at the XbaI site (Suzuki *et al.*, 2004). A nucleotide sequence for a 12-amino-acid (GGGSGGGSGGGS) linker was then inserted into the KpnI sites of pCI vectors that contained chimeric MPT51 DNA. The chimeric DNA constructs thus prepared were designated *HSP70F-MPT51*, *HSP70N-MPT51*, and *HSP70C-MPT51*. As a control, *HSP70F* was amplified by PCR using a primer set as follows: 5′-TATGAATTCACCATGGCTCGTGCGGTCG GG-3′ (forward, an underline indicates the EcoRI site) and 5′-AATGGTACCTCACTTGGCCTCCCGGCCGT-3′ (reverse, an underline indicates the KpnI site). The PCR product was purified and cloned into the EcoRI/KpnI sites of the pCI vector. The pCI plasmids containing these constructs were propagated in *Escherichia coli* strain XL1-Blue (Stratagene, La Jolla, CA) and purified by EndoFree Plasmid Maxi Kit (Qiagen GmbH, Hilden, Germany). The concentration of endotoxin was tested using the Endospecy ES-24S kit and the Toxicolor DIA kit (both from Seikagaku Biobusiness Corporation, Tokyo, Japan), and all plasmid solutions were found to contain < 0.1 EU endotoxin μg^{-1} DNA.

Preparation of fusion proteins

For protein preparation, *MPT51*, *HSP70F-MPT51*, *HSP70N-MPT51*, and *HSP70C-MPT51* were 6 × histidine-tagged by PCR using the corresponding forward primers listed above and a reverse primer (CAAGCTTTTAATGATGATGATGATGATGGCGGATCGCACCGACGATAT) containing nucleotide sequences for the extreme C-terminal of MPT51, the histidine-tag (double underlined), and the HindIII site (underlined). The PCR products were purified and cloned into the EcoRI/HindIII sites of the pRSET expression vector (Invitrogen, Carlsbad, CA). *Escherichia coli* JM109 competent cells were transformed with the expression vectors, and proteins were induced according to the manufacturer's instructions. Proteins were extracted and purified by Ni^{2+}-nitrilotriacetic acid (Ni-NTA) agarose (Qiagen GmbH) in the presence of 7 M urea, according to the manufacturer's instructions. Purified proteins were refolded by decreasing the concentration of urea while immobilized on the Ni-NTA matrix and then eluted by phosphate-buffered saline (PBS) (pH 7.4) containing 250 mM imidazole. The buffer was finally exchanged with PBS (pH 7.4) using a PD-10 desalting column (GE Healthcare, Uppsala, Sweden). The purity of recombinant proteins was checked by sodium dodecyl sulfate polyacrylamide gel electrophoresis (SDS-PAGE). The concentration of endotoxin was tested using the Endospecy ES-24S kit and the Toxicolor DIA kit, and recombinant protein solutions contained < 10 EU endotoxin mg^{-1} protein.

Preparation of anti-MPT51 monoclonal antibody (mAbs)

Anti-MPT51 mAbs were prepared as described previously (Harlow & Lane, 1988). Briefly, purified recombinant MPT51 protein (50 μg per mouse) was mixed with the RIBI Adjuvant System (Corixa, Hamilton, MT) and injected subcutaneously into BALB/c mice three times at 3-week intervals. Spleen cells from immunized mice were fused with SP2/0, and stably hybridized cells were selected using HAT medium (Invitrogen). Hybridomas that produced anti-MPT51 mAbs were screened by enzyme-linked immunosorbent assay (ELISA), and two clones (2B11F5 and 2D9H2) were established by limiting dilution. Both clones produced

anti-MPT51 mAbs of the IgG1 isotype, as determined using a Mouse Immunoglobulin Isotype Kit (BD Biosciences Pharmingen, San Diego, CA).

Western blotting detection of chimeric MPT51 proteins

HEK293T cells were transfected with pCI plasmids that encoded MPT51 DNA of various forms using FuGENE 6 (Roche Diagnostics GmbH, Mannheim, Germany). Cells were collected 24 h after transfection and lysed in the radioimmunoprecipitation assay buffer (25 mM Tris-HCl, pH 7.6, 150 mM NaCl, 1% NP-40, 1% sodium deoxycholate, 0.1% SDS), and Western blotting was performed with mouse anti-MPT51 mAb (from 2B11F5), HRP-conjugated goat anti-mouse immunoglobulins (Zymed Laboratories/Invitrogen), and West Pico Chemiluminescent Substrate (Pierce, Rockford, IL).

Animals and immunization

Female BALB/c and C57BL/6 mice (between 7 and 9 weeks of age) were purchased from Japan SLC (Hamamatsu, Japan) and maintained at the Institute for Experimental Animals, Hamamatsu University School of Medicine. All animal experiments were performed according to the Guidelines for Animal Experimentation, Hamamatsu University School of Medicine.

Mice were epidermally immunized with plasmids (2 μg per mouse per immunization) using the Helios gene gun system (Bio-Rad Laboratories, Hercules, CA) as described previously (Suzuki *et al.*, 2004) or recombinant proteins (50 μg per mouse) emulsified with incomplete Freund's adjuvant (Difco Laboratories/BD Diagnostic Systems, Sparks, MD) by injecting subcutaneously three times at 10-day intervals.

ELISA for interferon-γ (IFN-γ)

Two weeks after the last immunization, spleen cells from immunized BALB/c and C57BL/6 mice were cultured in a 96-well plate (1×10^6/0.2 cells mL^{-1}) in the presence of MPT51 peptides (1 μM) for 2 and 4 days, respectively. Antigenic peptides P24-32 and P171-190 (a dominant H2-A^b-restricted epitope) (Suzuki *et al.*, 2004) were used for CD8+ and CD4+ T-cell stimulation, respectively. For protein immunization, spleen cells from immunized or naïve C57BL/6 mice were stimulated with an antigenic peptide P171-190 (1 μM) for 4 days as described above. The IFN-γ concentration of the culture supernatants was determined by a sandwich ELISA as described previously (Yoshida *et al.*, 1995).

Preparation of total RNA and semi-quantitative reverse transcriptase (RT)-PCR

Two weeks after the last immunization, spleen cells from immunized C57BL/6 mice were cultured in a 12-well plate (1×10^7 cells mL^{-1} per well) in the presence of 1 μM MPT51 peptide (P171-190) for 16 h. Total RNA was prepared using ISOGEN (Nippon Gene, Tokyo, Japan), and semi-quantitative RT-PCR was performed as described previously (Uchijima *et al.*, 2005) using primers as follows:

inducible nitric oxide synthase (iNOS)
5′-TACAAGATGACCCTAAGAGT-3′ (forward)
5′-ACATGGCCGAGCGTCAAAGA-3′ (reverse)
IFN-γ
5′-TCTGAGACAATAAACGCTAC-3′ (forward)
5′-GAATCAGCAGCGACTCCTTT-3′ (reverse)
glycerol-3-phosphate dehydrogenase (G3PDH)
5′-ACCACAGTCCAT CCATCAC-3′ (forward)
5′-TCCACCACCCTGTTGCTGTA-3′ (reverse)

Statistical analysis

Statistical analyses were performed using STATVIEW-J 5.0 statistics program (SAS Institute Inc., Cary, NC). The Mann–Whitney test was used to calculate *P*-values.

Results

Enhancement of MPT51-specific T-cell responses by full-length HSP70

We first examined the enhancing effect of full-length HSP70 (HSP70F) for the induction of MPT51-specific T-cell responses. Because MPT51 induces only CD4+ or CD8+ T-cell response in C57BL/6 or BALB/c, respectively (Suzuki *et al.*, 2004), we used both strains to investigate their corresponding T-cell responses. C57BL/6 and BALB/c mice were immunized with a fusion gene of HSP70F and MPT51 (*HSP70F-MPT51*) or *MPT51* using the Helios gene gun system. Spleen cells from immunized C57BL/6 and BALB/c mice were used for IFN-γ production assays of CD4+ and CD8+ T cells, respectively, in response to corresponding antigenic peptides. CD4+ T cells from C57BL/6 mice immunized with *HSP70F-MPT51* produced a significantly higher amount of IFN-γ than those immunized with *MPT51* (Fig. 1). The addition of HSP70F to MPT51 did not show a significant enhancing effect on the antigen-specific CD8+ response, although CD8+ T cells from BALB/c mice immunized with *HSP70F-MPT51* showed a slightly higher IFN-γ production than those immunized with *MPT51*. Immunization with HSP70F DNA alone did not induce MPT51-specific immune responses in C57BL/6 and BALB/c mice, and the amounts of IFN-γ production from spleen cells of immunized mice in response to corresponding

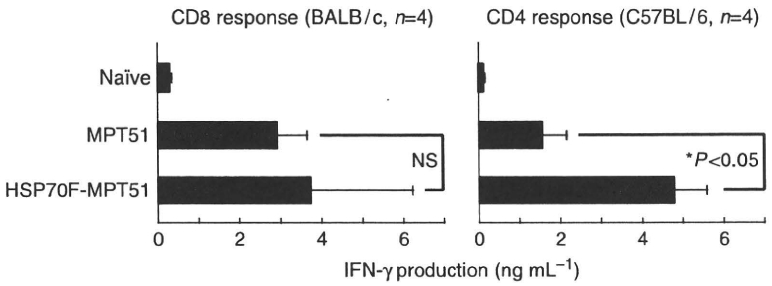

Fig. 1. Enhancing effect of HSP70 conjugation on MPT51-specific immune response. BALB/c (for CD8+ T-cell response) and C57BL/6 (for CD4+ T-cell response) mice were immunized with plasmids that encoded *HSP70F-MPT51* or *MPT51* alone, and their spleen cells were stimulated with the corresponding antigenic peptides. The IFN-γ concentration of the culture supernatants was determined by ELISA. The results of four mice per group are presented as mean ± SD. NS, not significant; $*P < 0.05$. IFN-γ productions from unstimulated spleen cells were nearly undetectable in all groups.

peptides were similar to those of naïve mice (data not shown). In contrast to IFN-γ production, *HSP70F-MPT51* showed no enhancing effect on MPT51-specific interleukin-4 (IL-4) production in both strains, although spleen cells from both strains similarly produced IL-4 in response to anti-CD3 mAb stimulation (data not shown). Taken together, the addition of HSP70 to MPT51 enhanced antigen-specific T-helper cell type 1 (Th1), but not Th2 responses.

Identification of the domain of HSP70 responsible for its enhancing effect on MPT51-specific T-cell response

Because HSP70 comprises two major domains, that is, the N-terminal ATPase domain (44 kDa) and the C-terminal peptide-binding domain (27 kDa), we next attempted to identify the domain that was responsible for the enhancement of the MPT51-specific T-cell response. For this purpose, we prepared additional fusion genes, *HSP70N-MPT51* and *HSP70C-MPT51* (Fig. 2a).

Before immunization, 293 T cells were transfected transiently with plasmids that encoded these chimeric MPT51 DNAs, to confirm the protein expression *in vitro*. Both fusion proteins, as well as HSP70F-MPT51 and MPT51, were detected at around the expected molecular sizes by Western blotting with anti-MPT51 mAb (Fig. 2b), indicating the proper amino acid sequences of expressed proteins.

BALB/c and C57BL/6 mice were then immunized with the plasmids containing *HSP70N-MPT51*, *HSP70C-MPT51*, or *MPT51* by gene-gun and their spleen cells were tested for MPT51-specific T-cell responses. A stronger IFN-γ production from CD4+ T cells was induced by *HSP70C-MPT51* compared with that by *HSP70N-MPT51* and *MPT51* alone (Fig. 3). However, *HSP70C-MPT51* showed no enhancing effect on MPT51-specific IL-4 production (data not shown). Although the CD4+ T-cell response induced by *HSP70N-MPT51* seemed stronger than that induced by *MPT51*, the difference was not statistically significant. In contrast, the addition of either HSP70N or HSP70C did not have any effect on the induction of CD8+ T-cell responses, which confirmed the results with HSP70F. The enhancing effect of HSP70C was confirmed by semi-quantitative RT-PCR (Fig. 4). The expression of mRNA for IFN-γ was increased considerably, which resulted in the upregulation of mRNA for iNOS, probably in APCs. These results together indicate that the C-terminal domain of *M. tuberculosis* HSP70 contributes to the enhancement of antigen-specific Th1 responses.

Induction of MPT51-specific CD4+ T-cell responses by MPT51-HSP70 fusion proteins

We finally prepared fusion MPT51 proteins and examined their effects on the induction of MPT51-specific CD4+ T-cell responses. Although SDS-PAGE analysis showed all Ni-NTA-purified proteins to have molecular sizes slightly smaller than those algorithmically expected (Fig. 5a), they were confirmed to have proper amino acid sequences by sequencing analyses (data not shown). When mice were immunized with these recombinant proteins, HSP70F-MPT51 and HSP70C-MPT51 again induced stronger immune responses than HSP70N-MPT51 and MPT51, and the effect of HSP70C-MPT51 was superior to that of HSP70F-MPT51 (Fig. 5b). These results confirm the evidence obtained by DNA vaccination that *M. tuberculosis* HSP70, especially its C-terminal domain, facilitates the induction of antigen-specific CD4+ T-cell responses.

Discussion

In DNA vaccines, the plasmid DNA is delivered into somatic cells (such as keratinocytes or myocytes) and professional APCs (such as DCs), but the former cells serve as a predominant reservoir for antigen (Gurunathan *et al.*, 2000; Kutzler & Weiner, 2008). DNA vaccines express a low amount of antigen at the restricted site of inoculation, and the frequency of DC bearing vaccinated DNA is very low